


RESEARCH

Open Access



Modified homotopy perturbation method and its application to analytical solitons of fractional-order Korteweg–de Vries equation

Adedapo Ismaila Alaje^{*} , Morufu Oyedunsi Olayiwola, Kamilu Adewale Adedokun, Joseph Adeleke Adedeji and Asimiyu Olamilekan Oladapo

Abstract

Background: Experimentally brought to light by Russell and hypothetically explained by Korteweg–de Vries, the KDV equation has drawn the attention of several mathematicians and physicists because of its extreme substantial structure in describing nonlinear evolution equations governing the propagation of weakly dispersive and nonlinear waves. Due to the prevalent nature and application of solitary waves in nonlinear dynamics, we discuss the soliton solution and application of the fractional-order Korteweg–de Vries (KDV) equation using a new analytical approach named the “Modified initial guess homotopy perturbation.”

Results: We established the proposed technique by coupling a power series function of arbitrary order with the renowned homotopy perturbation method. The convergence of the method is proved using the Banach fixed point theorem. The methodology was demonstrated with a generalized KDV equation, and we applied it to solve linear and nonlinear fractional-order Korteweg–de Vries equations, which are in Caputo sense. The method’s applicability and effectiveness were established as a feasible series of arbitrary orders that accelerate quickly to the exact solution at an integer order and are obtained as solutions. Numerical simulations were conducted to investigate the effect of Caputo fractional-order derivatives in the dispersion and propagation of water waves by varying the order α on the $[0, 1]$ interval. Comparative analysis of the simulation results, which were presented graphically and discussed, reveals that the degree of freedom of the Caputo fractional-order derivative is vital to controlling the magnitude of environmental hazards associated with water waves when adjusted.

Conclusion: The proposed method is recommended for obtaining convergent series solutions to fractional-order partial differential equations. We suggested that applied mathematicians and physicists investigate this work to better understand the impact of the degree of freedom posed by Caputo fractional-order derivatives in wave dispersion and propagation, as physical applications can help divert wave-related environmental hazards.

Keywords: Korteweg–de Vries, Modified homotopy perturbation method, Caputo derivative, Wave propagation

1 Background

When waves advance into the region of shallow water, they tend to be affected by the ocean bottom. This leads to the disruption of free water in orbital motion, and

the water molecules in the orbital motion can no longer return to their initial position. In turn, environmental hazards such as coastal erosion and the tsunami wave described in [19] are caused by this phenomenon, which often leads to loss of land and damage to the properties of people living in coastal regions [43]. Sailors do simulate the consequences of shallow water waves as it increases the realism of the virtual ocean scene and also supplies accurate parameters to the ship maneuvering model [3].

*Correspondence: adedapo.alaje@uniosun.edu.ng

Department of Mathematical Sciences, Osun State University, Osogbo, Nigeria

The intensity of a water wave can be measured by its dispersion. This dispersion is either caused by the interaction of the wave with the transmitting medium or by the geometry and physical constraints [32]. Different mathematical models have been developed to study the impact, significance, and ways of controlling water waves. Among these models are the Boussinesq wave model and the shallow water wave model in [37] and [41], respectively.

Of interest is the dispersive partial differential equation named the Korteweg–de Vries (KDV) equation [26]. It governs weakly and nonlinearly interacting radio waves above 1 km in wavelength with a frequency of 300 kHz traveling in canals of shallow water [28]. The general form of this equation can be found in [8, 31]. The homogenous Korteweg–de Vries equation [7, 36], which described the mathematical model of solitary water waves in a shallow water domain, was coined by Kruskal and Zabusky [2, 9, 17]. Unlike the shallow water equation (which does not take into account the frequency of wave dispersion) and the Boussinesq wave equation (where the use of wave reflections is limited), the Korteweg–de Vries equation can be applied to waves propagating in a single direction that have both frequency and amplitude of dispersion. A recent study in [14] discussed the behavior of different types of traveling waves in the solution of relativistic wave equations associated with the notable Schrödinger equation.

Although the analytic solution of this problem is often not feasible to obtain, an analytic study on the solution of a third-order dispersive partial differential equation was conducted in [13]. The Laplace–Adomian decomposition method (LADM) was applied in [27] to obtain the analytical solutions of third-order dispersive fractional partial differential equations. The fractional derivatives are in Caputo sense, and the approximate solution obtained converges directly to the exact solutions. Some semi-analytic techniques have also been employed to solve this well-known equation, one of which is in [39], where the Laplace–Adomian decomposition method (LADM), differential transform method (DTM), homotopy perturbation method (HPM), and homotopy perturbation transform method (HPTM) were applied to obtain the solution of linearized dispersive KDV equations. Other numerical techniques, such as the variational iteration method (VIM) proposed by [33], were applied in [6] to solve the higher-order nonlinear KDV equation, and its modification was applied in [7] to obtain the analytical solution of this equation.

Lately, fractional calculus has been an area of interest for modern researchers. This is due to the higher degree of freedom and more realistic behavior exhibited by physical problems governed by it. There exists a diverse set of fractional operators; these consist of the

Riemann–Liouville [44], Caputo [11], Caputo–Fabrizio [42], and Antagana–Baleanu [12] operators. These operators are often used as generalized tools for investigating diverse phenomena with a non-local kernel, such as fractal and chaotic phenomena with long-range memory. The strength and limitations of these concepts can be found in [44]. Several authors have proposed potent mathematical models capable of simulating chaotic and fractal systems. An example is a study presented in [29] where the numerical solutions and synchronization of a variable-order fractional chaotic system were conducted. A research study on the robust study of listeriosis disease was carried out in [38]. Their study implemented the use of fractal fractional operators to conduct their analysis. Their results show that these operators are productive for the purpose of their study.

Water waves are one of the many non-localized physical phenomena described by natural processes found around us. The sequencing pattern of the motion caused by water waves is often associated with fractals [16]. Research presented in [25] shows that modeling of these patterns cannot be carried out with ordinary classical derivatives that are localized. They claimed that the long-established differentiation technique (integer-order derivatives) is local and that using it to describe physical phenomena with unbounded disparities would be inappropriate because the impact of a larger neighborhood could not be ignored. They discussed that a fractional derivative is a global operator, whose properties thrive on examining the impacts of a larger neighborhood ignored by the local operator as it creates the likelihood of several possibilities for backward and forward motion of waves. They concluded that a non-localized derivative such as the Caputo fractional-order derivative should be employed in the modeling of water waves. The properties and application of these non-localized derivatives were applied in [15], where hybrid Caputo fractional modeling for thermostats with hybrid boundary value conditions was carried out. Investigation of a new version of HIV mathematical model using a new approach to fractional derivatives (Caputo–Fabrizio) was applied in [45]. This Caputo–Fabrizio fractional derivative was also applied in [1] to a mathematical theoretical study for the Rubella disease model, as they stated that fractional derivatives, such as Caputo and Riemann derivatives, have their own limitations because their kernel is singular and they cannot be applied to describe the memory effect of the physical system applicable to their problem.

To obtain the solutions of the fractional-order Korteweg–de Vries equation, researchers in [18] successfully applied the fractional differential transform method (FDTM) and modified differential transform method (MDTM) to obtain the solution of

the third-order dispersive partial differential equation. In [20], the Laplace–Adomian decomposition method was applied to obtain the solution of the fractional-order model of measles, and in [21], this same method was applied to obtain the numerical solution of the fractional-order smoking model.

In this paper, an initial guess technique applied in [4, 5, 40] is modified to be of arbitrary order in a Caputo sense. We coupled it with the homotopy perturbation method introduced in [22, 23, 34, 35] to suit the computation of an approximate solution of the fractional-order Korteweg–de Vries equation of the form:

$$u_t^\alpha(x, t) + \xi u(x, t)u_x(x, t) + \gamma u_{xxx}(x, t) = 0, \quad 0 < \alpha \leq 1 \tag{1}$$

subject to the initial condition:

$$u(x, 0) = \phi(x). \tag{2}$$

$u(x, t)$ is a function of real variables which denotes the wave elongation at space x and time t , respectively. $u(x, t)u_x(x, t)$ is the nonlinear term, $u_{xxx}(x, t)$ represents the direction of the wave dispersion, and ξ, γ are arbitrary constants put in place to obtain a uniformly propagating wave solution.

2 Methods

2.1 Preliminaries

Here, we state some fundamental properties of fractional calculus applicable in this paper.

Definition 1 A real function $\phi(t)$, $t > 0$, is said to be in the space C_μ , $\mu \in R$ if there exist a real number $m > \mu$ such that $\phi(t) = t^m \phi_1(t)$, where $\phi_1(t) \in C(0, \infty)$, and it is said to be in the space C_μ^n if and only if $\phi^{(n)} \in C_\mu$, $n \in N$.

Definition 2 The Riemann–Liouville fractional integration of order $\eta \geq 0$ for a real positive function $\phi(t) \in C_\mu$, $\mu \geq -1$ $t > 0$ is defined as:

$$I^\eta \phi(t) = \frac{1}{\Gamma(\eta)} \int_0^t (t-x)^{\eta-1} \phi(x) dx.$$

The following properties hold for fractional integral operator I^η for $\phi(t) \in C_\mu$, $\mu \geq -1$ $\eta, \alpha \geq 0$ and $\beta \geq -1$:

1. $I^\eta I^\alpha \phi(t) = I^{\eta+\alpha} \phi(t)$,
2. $I^\eta I^\alpha \phi(t) = I^\alpha I^\eta \phi(t)$,
3. $I^\eta t^\beta = \frac{\Gamma(\beta+1)}{\Gamma(\eta+\beta+1)} t^{\eta+\beta}$.

Definition 3 The Caputo fractional derivative of a positive real function $\phi(t) \in C_\mu$ is mathematically expressed as

$$D^\eta \phi(t) = \frac{1}{\Gamma(n-\eta)} \int_0^t (t-x)^{n-\eta-1} \phi^{(n)}(x) dx, \quad n-1 < \eta \leq n, n \in N.$$

The fractional integration of Caputo derivative for $n-1 < \eta \leq n$, $n \in N$, $\phi \in C_{-1}^n$, $\mu \geq -1$ is:

$$I^n D^\eta \phi(t) = \phi(t) - \sum_{k=0}^{n-1} \phi^{(k)}(0) \frac{t^k}{k!}.$$

2.2 Homotopy perturbation method

The fundamental scheme of He’s homotopy perturbation method can be illustrated by considering the general nonlinear differential equation of the form:

$$D(u) - f(\omega) = 0, \quad \omega \in \Omega. \tag{3}$$

subject to the boundary condition:

$$\beta(u, u_n) = 0, \quad \omega \in \Gamma. \tag{4}$$

The general differential operator is denoted by D and the boundary operator by β . $f(\omega)$ is an analytic function, and Γ is the boundary operator in the domain Ω . The operator D is separable into two parts:

$$D^\alpha(u) = \ell(u) + \eta(u). \tag{5}$$

The functions ℓ and η represent the linear and nonlinear operator, respectively. Substituting Eq. (5) into Eq. (3) yields

$$\ell(u) + \eta(u) - f(\omega) = 0. \tag{6}$$

A homotopy can be constructed for Eq. (6):

$$H(v, p) = (1-p)[\ell(v) - \ell(u_0)] + p[D(v) - f(\omega)] = 0; \tag{7}$$

simplifying Eq. (7) yields

$$H(v, p) = \ell(v) - \ell(u_0) + p\ell[v_0] + p[\eta(v) - f(\omega)] = 0. \tag{8}$$

where p is an embedded parameter which undergoes deformation process of changing from 0 to 1: When $p = 0$,

$$H(v, 0) = \ell(v) - \ell(u_0) = 0, \tag{9}$$

and at $p = 1$,

$$H(v, 1) = D(v) - f(\omega) = 0. \tag{10}$$

Proof Consider the Picard sequence $m_{s+1} = \tau(m_s) \subseteq Y$ we want to show that m_s is convergent in Y for all $r \geq s$ $\|m_s - m_r\| \leq \|m_s - m_{s+1}\| + \|m_{s+1} - m_{s+2}\| + \|m_{s+2} - m_{s+3}\| + \dots + \|m_{s-1} - m_r\|$.

We define the proof by applying mathematical induction on the contractive property of (C):

$$\|m_s - m_{s+1}\| \leq \varepsilon^s \|m_0 - m_1\|. \quad \text{By implication,}$$

$$\lim_{r \rightarrow \infty} \|m_s - m_r\| \leq \frac{\varepsilon^s}{1 + \varepsilon} \|m_0 - m_1\| = 0 \text{ as } s \rightarrow \infty.$$

This proves that (m_s) is convergent in Y and through completeness of Y , we can find $\omega \in Y: \lim_{s \rightarrow \infty} (m_s) = \omega \in Y$. Clearly, the continuity of τ is ensured by the contraction (C). Thus, $\omega = \lim_{s \rightarrow \infty} m_{s+1} = m_r$.

3 Application and results

3.1 Example 1

Consider the dispersive KDV equation

$$\frac{\partial^\alpha \mu(x, t)}{\partial t^\alpha} - 6\mu(x, t) \frac{\partial \mu(x, t)}{\partial x} + \frac{\partial^3 \mu(x, t)}{\partial x^3} = 0, \quad (24)$$

subject to the initial condition:

$$\mu(x, 0) = \frac{x - 2}{12}. \quad (25)$$

By modified initial guess homotopy perturbation method,

$$\mu(x, t) = \mu(x, 0) + \lambda_1 t^\alpha + \dots \quad (26)$$

Equation (24) is evaluated using the following derivatives in Eq. (27)

$$\frac{\partial^\alpha \mu(x, t)}{\partial t^\alpha} = \lambda_1 \Gamma(\alpha + 1), \quad \frac{\partial \mu(x, t)}{\partial x} = \frac{1}{12}, \quad \frac{\partial^3 \mu(x, t)}{\partial x^3} = 0, \quad (27)$$

such that at $t = 0$,

$$\lambda_1 = \frac{(x - 2)}{24\Gamma(\alpha + 1)}. \quad (28)$$

Therefore,

$$\mu_4(x, t) = \left(\frac{(x - 2)4(\Gamma(1 + \alpha))^2\Gamma(1 + 2\alpha) + (\Gamma(1 + 2\alpha))^2 + 2\Gamma(1 + \alpha)\Gamma(1 + 3\alpha)}{96(\Gamma(1 + \alpha))^2\Gamma(1 + 2\alpha)\Gamma(1 + 4\alpha)} t^{4\alpha} \right), \quad (38)$$

$$\mu_1(x, t) = \frac{(x - 2)}{24\Gamma(\alpha + 1)} t^\alpha. \quad (29)$$

Constructing a homotopy for Eq. (24),

$$(1 - p) \frac{\partial^\alpha \mu(x, t)}{\partial t^\alpha} + p \left(\frac{\partial^\alpha \mu(x, t)}{\partial t^\alpha} - \mu(x, t) \frac{\partial \mu(x, t)}{\partial x} + \frac{\partial^3 \mu(x, t)}{\partial x^3} \right) = 0; \quad (30)$$

simplifying Eq. (30),

$$\frac{\partial^\alpha \mu(x, t)}{\partial t^\alpha} + p \left(-6\mu(x, t) \frac{\partial \mu(x, t)}{\partial x} + \frac{\partial^3 \mu(x, t)}{\partial x^3} \right) = 0. \quad (31)$$

We can assume a series solution of the form:

$$\mu(x, t) = \mu_0(x, t) + p\mu_1(x, t) + p^2\mu_2(x, t) + \dots + p^n\mu_n(x, t). \quad (32)$$

Substituting Eq. (32) into Eq. (31) and equating coefficients of equal powers of p^n , $n \geq 2$;

$$p^2 : \frac{\partial^\alpha \mu_2(x, t)}{\partial t^\alpha} - 6 \left(\mu_0(x, t) \frac{\partial \mu_1(x, t)}{\partial x} + \mu_1(x, t) \frac{\partial \mu_0(x, t)}{\partial x} \right) + \frac{\partial^3 \mu_0(x, t)}{\partial x^3} = 0, \quad (33)$$

$$p^3 : \frac{\partial^\alpha \mu_3(x, t)}{\partial t^\alpha} - 6 \left(\mu_0(x, t) \frac{\partial \mu_2(x, t)}{\partial x} + \mu_1(x, t) \frac{\partial \mu_1(x, t)}{\partial x} + \mu_2(x, t) \frac{\partial \mu_0(x, t)}{\partial x} \right) + \frac{\partial^3 \mu_1(x, t)}{\partial x^3} = 0. \quad (34)$$

Evaluating Eq. (33) using $\mu_0(x, t)$ & $\mu_1(x, t)$,

$$\frac{\partial^\alpha \mu_2(x, t)}{\partial t^\alpha} - \frac{(x - 2)}{24\Gamma(\alpha + 1)} t^\alpha = 0 \Rightarrow \frac{\partial^\alpha \mu_2(x, t)}{\partial t^\alpha} = \frac{(x - 2)}{24\Gamma(\alpha + 1)} t^\alpha. \quad (35)$$

Applying operator I^α to both sides of Eq. (35),

$$\mu_2(x, t) = \frac{(x - 2)}{24\Gamma(2\alpha + 1)} t^{2\alpha}. \quad (36)$$

Repeating the iterative process,

$$\mu_3(x, t) = \left(\frac{(x - 2)4(\Gamma(1 + \alpha))^2 + \Gamma(1 + 2\alpha)}{96(\Gamma(1 + \alpha))^2\Gamma(1 + 3\alpha)} t^{3\alpha} \right), \quad (37)$$

and so on. The subsequent terms can be evaluated using MATHEMATICA 12 software package.

The approximate solution of Eq. (24) is therefore obtained as:

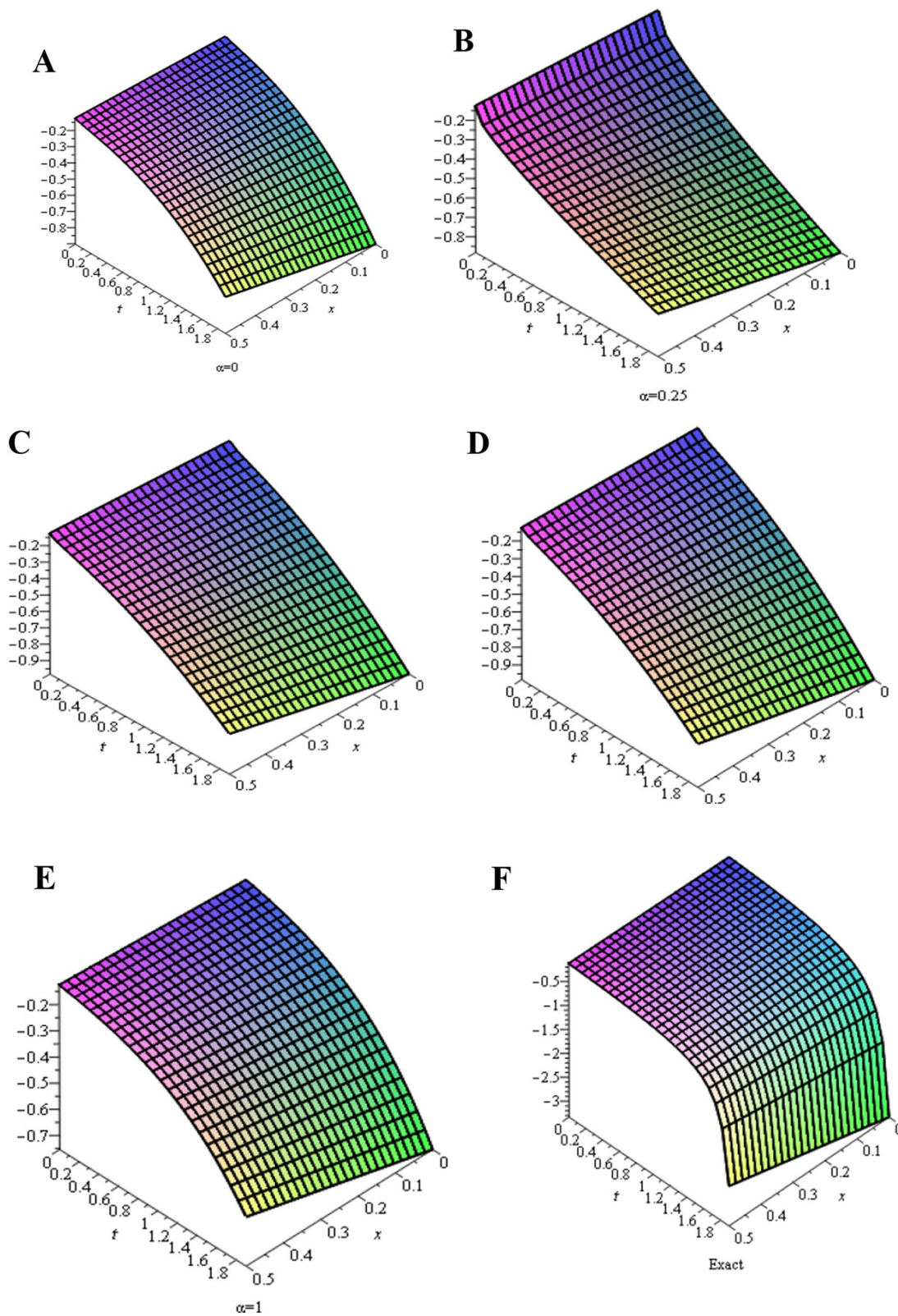


Fig. 1 A traveling solitary transitory wave, which preserves its form by not interacting with any local disturbances. The directions of wave propagation in space and time coordinate (x, t) at different degrees of freedom on the interval $0 \leq \alpha \leq 1$ were presented in **A–E**. **E** particularly reflects that the transitory wave tends to converge to the exact direction of the wave propagation presented in **F** at an integer order

$$\mu_n(x, t) = \left. \begin{aligned} &\frac{x-2}{12} + \frac{(x-2)}{24\Gamma(\alpha+1)}t^\alpha + \frac{(x-2)}{24\Gamma(2\alpha+1)}t^{2\alpha} + \frac{(x-2)4(\Gamma(1+\alpha))^2 + \Gamma(1+2\alpha)}{96(\Gamma(1+\alpha))^2\Gamma(1+3\alpha)}t^{3\alpha} \\ &\frac{(x-2)4(\Gamma(1+\alpha))^2\Gamma(1+2\alpha) + (\Gamma(1+2\alpha))^2 + 2\Gamma(1+\alpha)\Gamma(1+3\alpha)}{96(\Gamma(1+\alpha))^2\Gamma(1+2\alpha)\Gamma(1+4\alpha)}t^{4\alpha} \end{aligned} \right\} \quad (39)$$

When $\alpha = 1$,

$$\mu_n(x, t) = \frac{(x-2)}{12} + \frac{(x-2)t}{24} + \frac{(x-2)t^2}{48} + \frac{(x-2)t^3}{96} + \frac{(x-2)t^4}{192} + \dots$$

And the closed form of the solution is

$$\lim_{n \rightarrow \infty} \mu_n(x, t) = \frac{x-2}{12-6t}$$

(Fig. 1, Table 1).

3.2 Convergence of Solution

Following the theorem of nonlinear mapping X , the convergence of modified initial guess homotopy perturbation method strictly relies on contraction X .

Thus, $\|\mu_0 - \mu_e\| = \left\| \frac{x-2}{12} - \frac{x-2}{12-6t} \right\| = \frac{1}{12} \left\| \frac{(x-2)t}{(t-2)} \right\|$. For $\frac{1}{2} < \kappa, 0 < \kappa < 1$,

$$\|\mu_1 - \mu_e\| = \|\mu_0 + \mu_1 - \mu_e\| = \left\| \frac{1}{24} \frac{(x-2)t^2}{(t-2)} \right\| \leq \kappa \|\mu_0 - \mu_e\|,$$

Table 1 Numerical results of problem one at an exact value $\alpha = 1$

t	Value of (x)	Numerical solution	Exact solution	Abs error
$t = 0$	0	-0.16667	-0.16667	0
	0.1	-0.1583333334	-0.1583333333	1×10^{-10}
	0.2	-0.1500000000	-0.1500000000	0
	0.3	-0.1416666667	-0.1416666667	0
	0.4	-0.1333333334	-0.1333333333	1×10^{-10}
$t = 0.2$	0	-0.1250000000	-0.1250000000	0
	0.1	-0.1851833335	-0.1851851852	0.0000018517
	0.2	-0.1759241666	-0.1759259259	0.0000017593
	0.3	-0.1666650000	-0.1666666667	0.0000016667
	0.4	-0.1574058335	-0.1574074074	0.0000015739
$t = 0.4$	0	-0.1481466666	-0.1481481481	0.0000014815
	0.1	-0.1388875000	-0.1388888889	0.0000013889
	0.2	-0.2082666667	-0.2083333334	0.0000666667
	0.3	-0.1978533334	-0.1979166667	0.0000633333
	0.4	-0.1874400000	-0.1875000001	0.0000600001
$t = 0.6$	0	-0.1770266667	-0.1770833334	0.0000566667
	0.1	-0.1666133334	-0.1666666667	0.0000533333
	0.2	-0.1562000000	-0.1562500000	0.0000500000
	0.3	-0.2375166667	-0.2380952380	0.0005785713
	0.4	-0.2256408334	-0.2261904761	0.0005496427
$t = 0.8$	0	-0.2137650000	-0.2142857142	0.0005207142
	0.1	-0.2018891667	-0.2023809523	0.0004917856
	0.2	-0.1900133334	-0.1904761904	0.0004628570
	0.3	-0.1781375000	-0.1785714285	0.0004339285
	0.4	-0.2749333335	-0.2777777778	0.0028444443
$t = 0.8$	0	-0.2611866666	-0.2638888889	0.0027022223
	0.1	-0.2474400000	-0.2500000000	0.0025600000
	0.2	-0.2336933335	-0.2361111111	0.0024177776
	0.3	-0.2199466666	-0.2222222222	0.0022755556
	0.4	-0.2062000000	-0.2083333334	0.0021333334

Table 1 (continued)

<i>t</i>	Value of (<i>x</i>)	Numerical solution	Exact solution	Abs error
<i>t</i> = 1.0	0	-0.3229166667	-0.3333333334	0.0104166667
	0.1	-0.3067708334	-0.3166666667	0.0098958333
	0.2	-0.2906250000	-0.3000000001	0.0093750001
	0.3	-0.2744791667	-0.2833333334	0.0088541667
	0.4	-0.2583333334	-0.2666666667	0.0083333333
<i>t</i> = 1.2	0	-0.2421875000	-0.2500000000	0.0078125000
	0.1	-0.3842666667	-0.4166666666	0.0323999999
	0.2	-0.3650533334	-0.3958333333	0.0307799999
	0.3	-0.3458400000	-0.3749999999	0.0291599999
	0.4	-0.3266266667	-0.3541666666	0.0275399999
<i>t</i> = 1.4	0	-0.3074133334	-0.3333333333	0.0259199999
	0.1	-0.2882000000	-0.3125000000	0.0243000000
	0.2	-0.4621833335	-0.5555555556	0.0933722221
	0.3	-0.4390741666	-0.5277777778	0.0887036112
	0.4	-0.4159650000	-0.5000000000	0.0840350000
<i>t</i> = 1.6	0	-0.3928558335	-0.4722222223	0.0793663888
	0.1	-0.3697466666	-0.4444444445	0.0746977779
	0.2	-0.3466375000	-0.4166666667	0.0700291667
	0.3	-0.5602666667	-0.8333333334	0.2730666667
	0.4	-0.5322533334	-0.7916666667	0.2594133333
<i>t</i> = 1.8	0	-0.5042400000	-0.7500000001	0.2457600001
	0.1	-0.4762266667	-0.7083333334	0.2321066667
	0.2	-0.4482133334	-0.6666666667	0.2184533333
	0.3	-0.4202000000	-0.6250000000	0.2048000000
	0.4	-0.6825166667	-1.6666666667	0.9841500003
<i>t</i> = 1.8	0.1	-0.6483908334	-1.5833333333	0.9349424996
	0.2	-0.6142650000	-1.5000000000	0.8857350000
	0.3	-0.5801391667	-1.4166666667	0.8365275003
	0.4	-0.5460133334	-1.3333333333	0.7873199996
	0.5	-0.5118875000	-1.2500000000	0.7381125000

Table shows the approximate solution, exact solution, and absolute errors computed at a time-varying level of *x*. We observed that the approximate result deviates from the exact solutions as the value increases. For example, the absolute error observed when *t* = 0 is of order $\times 10^{-10}$; at *t* = 1 the absolute error is in order of $\times 10^{-3}$ to $\times 10^{-2}$; and at *t* = 1.8 the absolute error is in order of $\times 10^{-1}$.

$$\begin{aligned} \|\mu_2 - \mu_e\| &= \|\mu_0 + \mu_1 + \mu_2 - \mu_e\| \\ &= \left\| \frac{1}{48} \frac{(x-2)t^3}{(t-2)} \right\| \leq \kappa^2 \|\mu_0 - \mu_e\|, \\ \|\mu_3 - \mu_e\| &= \|\mu_0 + \mu_1 + \mu_2 + \mu_3 - \mu_e\| \\ &= \left\| \frac{1}{96} \frac{(x-2)t^4}{(t-2)} \right\| \leq \kappa^3 \|\mu_0 - \mu_e\|, \\ \|\mu_n - \mu_e\| &= \|(\mu_0 + \mu_1 + \mu_2 + \dots + \mu_n) - \mu_e\| \\ &= \left\| \frac{1}{12 \cdot 2^n} \frac{(x-2)t^n}{(t-2)} \right\| \leq \kappa^n \|\mu_0 - \mu_e\|. \end{aligned}$$

Clearly, $\lim_{n \rightarrow \infty} \kappa^n = 0$; therefore, $\lim_{n \rightarrow \infty} \|\mu_n - \mu_e\| \leq \kappa^n \|\mu_0 - \mu_e\| = 0$. Thus, modified initial guess homotopy perturbation method agrees that $\mu_e = \lim_{n \rightarrow \infty} \mu_n(x, t) = \frac{x-2}{12-6t}$ which is the exact solution of the problem.

3.3 Problem 2

Consider the following linear homogenous KDV equation

$$\frac{\partial^\alpha \mu(x, t)}{\partial t^\alpha} + 7 \frac{\partial \mu(x, t)}{\partial x} + 6 \frac{\partial \mu(x, t)}{\partial x^3} = 0, \tag{40}$$

subject to the condition:

$$\mu(x, 0) = \cos(x). \tag{41}$$

such that

$$\mu_n(x, t) = \left. \begin{aligned} &\cos x \left(1 - \frac{t^{2\alpha}}{\Gamma(2\alpha+1)} + \frac{t^{4\alpha}}{\Gamma(4\alpha+1)} - \frac{t^{6\alpha}}{\Gamma(6\alpha+1)} + \frac{t^{8\alpha}}{\Gamma(8\alpha+1)} + \dots \right) \\ &+ \sin x \left(\frac{t^\alpha}{\Gamma(\alpha+1)} - \frac{t^{3\alpha}}{\Gamma(3\alpha+1)} + \frac{t^{5\alpha}}{\Gamma(5\alpha+1)} - \frac{\sin t^{7\alpha}}{\Gamma(7\alpha+1)} + \dots \right) \end{aligned} \right\} \tag{62}$$

When $\alpha = 1$,

$$\begin{aligned} \mu_n(x, t) = &\cos x \left(1 - \frac{t^2}{2} + \frac{t^4}{4!} - \frac{t^6}{6!} + \frac{t^8}{8!} + \dots \right) \\ &+ \sin x \left(t - \frac{t^3}{3!} + \frac{t^5}{5!} - \frac{t^7}{7!} + \dots \right) \end{aligned} \tag{63}$$

The modified method agrees that

$$\lim_{n \rightarrow \infty} \mu(x, t) = \mu(x, t). \tag{64}$$

By convergence, the exact solution is

$$\mu(x, t) = \cos x \cos t + \sin x \sin t.$$

In closed form (Fig. 2, Table 2),

$$\mu(x, t) = \cos(x - t).$$

3.4 Problem 3

Consider the following nonlinear homogenous KDV equation

$$\frac{\partial^\alpha \mu(x, t)}{\partial t^\alpha} + \xi u(x, t) \frac{\partial \mu(x, t)}{\partial x} + \frac{\partial^3 \mu(x, t)}{\partial x^3} = 0, \tag{65}$$

subject to the initial condition

$$\mu(x, 0) = x. \tag{66}$$

By modified initial guess homotopy perturbation method,

$$\mu(x, t) = \mu(x, 0) + \lambda_1 t^\alpha + \dots, \tag{67}$$

$$\frac{\partial^\alpha \mu(x, t)}{\partial t^\alpha} = \lambda_1 \Gamma(\alpha + 1), \quad \frac{\partial \mu(x, t)}{\partial x} = 1, \quad \frac{\partial^3 \mu(x, t)}{\partial x^3} = 0. \tag{68}$$

Evaluating Eq. (65) using Eq. (68),

$$\lambda_1 \Gamma(\alpha + 1) + \xi (x + \lambda t^\alpha) = 0. \tag{69}$$

$$\text{At } t = 0, \lambda_1 = \frac{-\xi x}{\Gamma(\alpha + 1)}. \tag{70}$$

Thus,

$$\mu_1(x, t) = \frac{-\xi x}{\Gamma(\alpha + 1)} t^\alpha \tag{71}$$

Constructing a homotopy for Eq. (65),

$$\begin{aligned} (1 - p) \frac{\partial^\alpha \mu(x, t)}{\partial t^\alpha} + p \left(\frac{\partial^\alpha \mu(x, t)}{\partial t^\alpha} \right. \\ \left. + \xi \mu(x, t) \frac{\partial \mu(x, t)}{\partial x} + \frac{\partial^3 \mu(x, t)}{\partial x^3} \right) = 0. \end{aligned} \tag{72}$$

Simplifying Eq. (72),

$$\frac{\partial^\alpha u(x, t)}{\partial t^\alpha} + p \left(\xi u(x, t) \frac{\partial u(x, t)}{\partial x} + \frac{\partial^3 u(x, t)}{\partial x^3} \right) = 0. \tag{73}$$

Substituting Eq. (50) into Eq. (73) and comparing coefficients of equal powers of p^n , $n \geq 2$.

$$\begin{aligned} p^2 : \frac{\partial^\alpha \mu_2(x, t)}{\partial t^\alpha} + \xi \left(\mu_0(x, t) \frac{\partial \mu_1(x, t)}{\partial x} \right. \\ \left. + \mu_1(x, t) \frac{\partial \mu_0(x, t)}{\partial x} \right) + \frac{\partial^3 \mu_0(x, t)}{\partial x^3} = 0, \end{aligned} \tag{74}$$

$$\begin{aligned} p^3 : \frac{\partial^\alpha \mu_3(x, t)}{\partial t^\alpha} + \xi \left(\mu_0(x, t) \frac{\partial \mu_2(x, t)}{\partial x} + \mu_1(x, t) \frac{\partial \mu_1(x, t)}{\partial x} \right. \\ \left. + \mu_2(x, t) \frac{\partial \mu_0(x, t)}{\partial x} \right) + \frac{\partial^3 \mu_1(x, t)}{\partial x^3} = 0, \end{aligned} \tag{75}$$

Evaluating Eq. (74) using $\mu_0(x, t)$ & $\mu_1(x, t)$,

(See figure on next page.)

Fig. 2 A traveling transverse wave which occurrence can be in the form of surface ripples on water. **A–H** show the different types of disturbance caused by the wave as $0 \leq \alpha \leq 1$. In **E**, it could be observed that proper crests are formed as $\alpha \rightarrow 1$. This means that the frequency of the disturbance will peak at an integer order. Figure **G** shows the behavioral pattern of the wave amplitude at different levels of α . The amplitude is periodically accelerated as α increases, and the highest amplitude is recorded as a unit for the wavelength considered. In **H**, the efficiency of the modified initial guess technique is proved as it produces an approximate result that converges to the exact solution

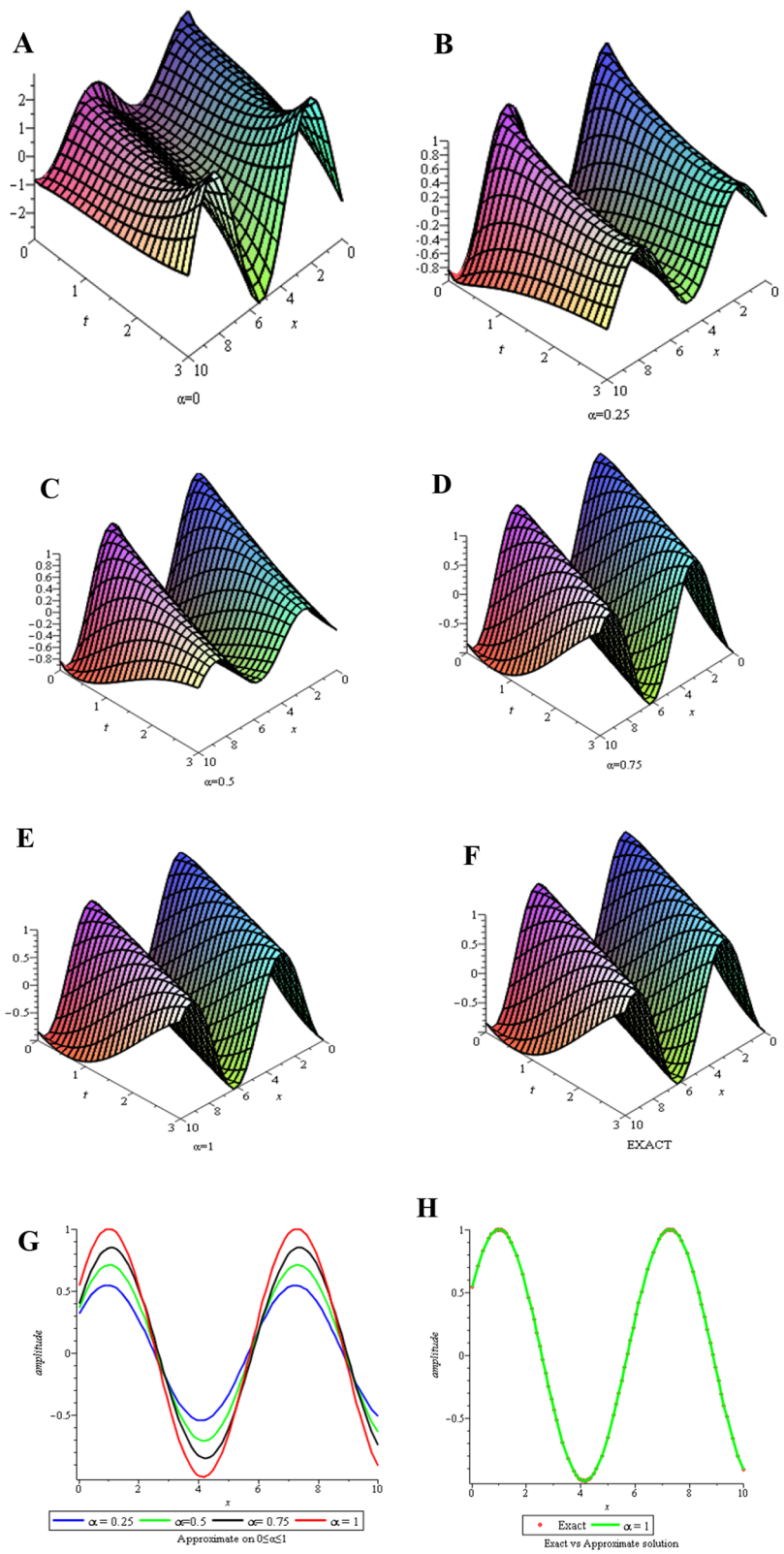


Fig. 2 (See legend on previous page.)

Table 2 Numerical results of problem two at an exact value $\alpha = 1$

t	Value of (x)	Numerical solution	Exact solution	Abs error
$t = 0$	0	1	1	0
	2	-0.4161468365	-0.4161468365	0
	4	-0.6536436209	-0.6536436209	0
	6	0.9601702867	0.9601702867	0
	8	-0.1455000338	-0.1455000338	0
	10	-0.8390715291	-0.8390715291	0
$t = 1$	0	0.5403023059	0.5403023059	$3.186028260 \times 10^{-11}$
	2	0.5403023057	0.5403023059	2×10^{-10}
	4	-0.9899924967	-0.9899924966	1×10^{-10}
	6	0.2836621855	0.2836621855	0
	8	0.7539022544	0.7539022543	1×10^{-10}
	10	-0.9111302620	0.9111302619	1×10^{-10}
$t = 2$	0	-0.4161468396	-0.4161468365	$3.05285761300 \times 10^{-9}$
	2	1.000000023	1	2.3×10^{-8}
	4	-0.4161468534	-0.4161468365	1.69×10^{-8}
	6	-0.6536436313	-0.6536436209	1.04×10^{-8}
	8	0.9601703110	0.9601702867	2.43×10^{-8}
	10	-0.1455000450	-0.1455000338	1.12×10^{-8}
$t = 3$	0	-0.9899944948	-0.9899924966	1.9982×10^{-6}
	2	0.5403127921	0.5403023059	104862×10^{-5}
	4	0.5402955751	0.5403023059	6.7308×10^{-6}
	6	-0.9899973839	0.9899924966	4.8873×10^{-6}
	8	0.2836729814	0.2836621855	1.07959×10^{-5}
	10	0.7538981557	0.7539022543	4.0986×10^{-6}

Table shows that the absolute error drastically increases as t increases. When $t = 0$, the absolute error is zero; when $t = 1$, the error ranges from $\times 10^{-11}$ to $\times 10^{-10}$; when $t = 2$, the error increases to an order which ranges from $\times 10^{-8}$ to $\times 10^{-9}$; and at $t = 3$, the absolute error alternate between $\times 10^{-6}$ to $\times 10^{-6}$.

$$\frac{\partial^\alpha \mu_2(x, t)}{\partial t^\alpha} - \frac{2\xi^2 x}{\Gamma(\alpha + 1)} t^\alpha = 0 \Rightarrow \frac{\partial^\alpha \mu_2(x, t)}{\partial t^\alpha} = \frac{2\xi^2 x}{\Gamma(\alpha + 1)} t^\alpha. \tag{76}$$

Applying operator I^α to Eq. (76),

$$\mu_2(x, t) = \frac{2\xi^2 x}{\Gamma(\alpha + 2)} t^{\alpha+1}. \tag{77}$$

Subsequently,

$$\mu_3(x, t) = - \left(\frac{\xi^3 x \Gamma(1 + 2\alpha)}{(\Gamma(1 + \alpha))^2 \Gamma(1 + 3\alpha)} t^{3\alpha} + \frac{4\xi^3 x}{\Gamma(2 + 2\alpha)} t^{1+2\alpha} \right) \tag{78}$$

and so on. The approximate solution is:

$$\mu_n(x, t) = x - \frac{-\xi x}{\Gamma(\alpha + 1)} t^\alpha + \frac{2\xi^2 x}{\Gamma(\alpha + 2)} t^{\alpha+1} - \left(\frac{\xi^3 x \Gamma(1 + 2\alpha)}{(\Gamma(1 + \alpha))^2 \Gamma(1 + 3\alpha)} t^{3\alpha} + \frac{4\xi^3 x}{\Gamma(2 + 2\alpha)} t^{1+2\alpha} \right) + \dots \tag{79}$$

When $\alpha = 1$, the integer solution is:

$$\mu_n(x, t) = x - tx\xi + t^2\xi^2x - t^3\xi^3x + \dots \tag{80}$$

The modified method agrees that

(See figure on next page.)
Fig. 3 A comprehensive clarification of the interference caused by wave propagation in the given domain of shallow water with a depth of 7 m and a width of 0.1 m. **B–H** depict the swirling direction of the wave as the degree of freedom increases. It was observed that the fluid tends to undergo less turbulence when hit by the wave at a lower level of α . **G** interprets the convergence of fractional order to integer order, and **H** is employed to show the accuracy of the method applied. To a great extent, it was observed that the approximate solution agrees with the exact solution

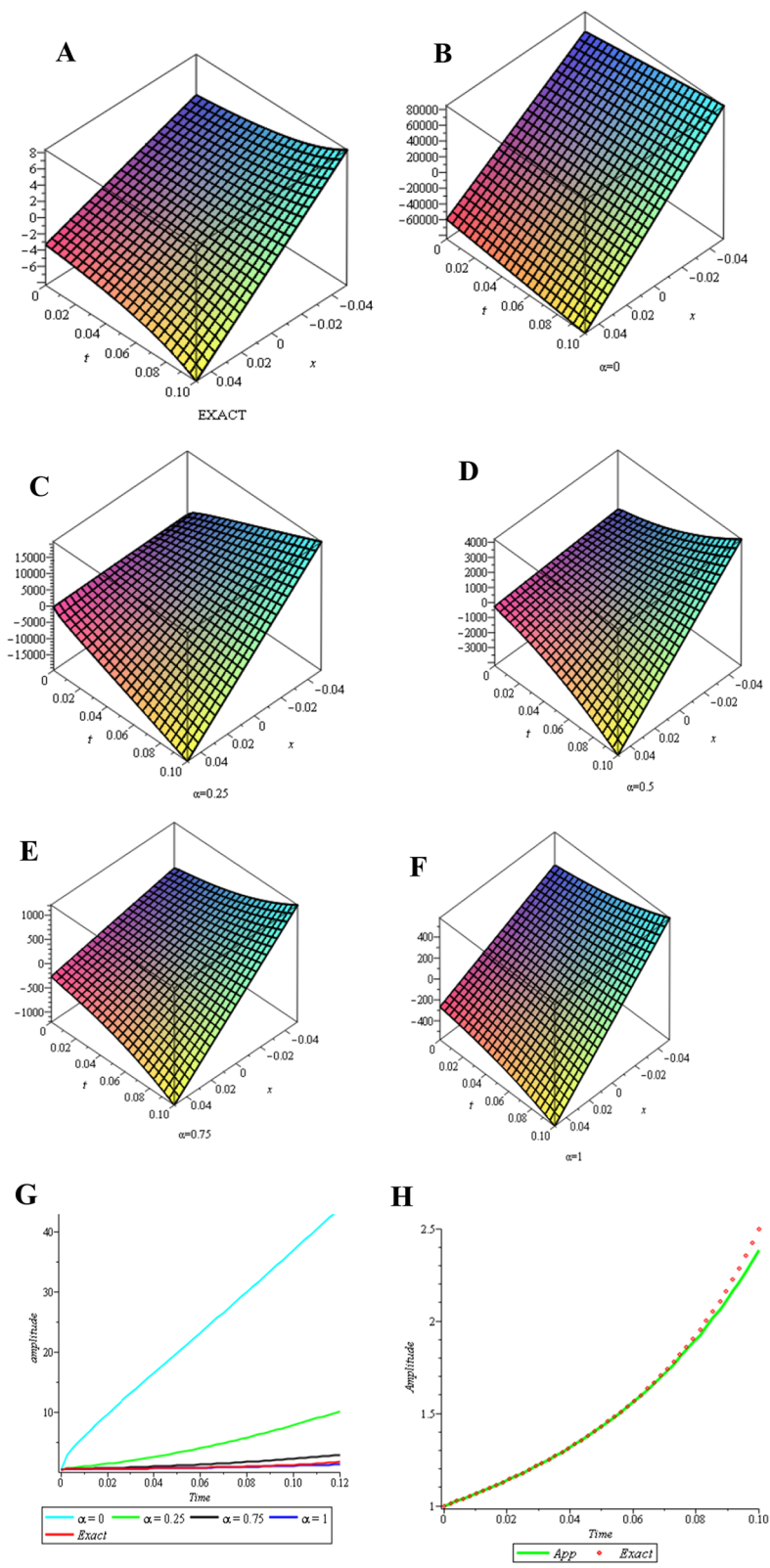


Fig. 3 (See legend on previous page.)

Table 3 Numerical results of problem three at an exact value $\alpha = 1$

t	Value of (x)	Numerical solution	Exact solution	Abs error
$t = 0$	-0.04	2.668682966	2.668682966	0
	-0.02	1.334341483	1.334341483	0
	0	0	0	0
	0.02	-1.334341483	-1.334341483	0
	0.04	-2.668682966	-2.668682966	0
$t = 0.02$	-0.04	3.031965441	3.032594279	0.000628838
	-0.02	1.515982720	1.516297139	0.000314419
	0	0	0	0
	0.02	-1.515982720	-1.516297139	0.000314419
	0.04	-3.031965441	-3.032594279	0.000628838
$t = 0.04$	-0.04	3.499774890	3.511424956	0.011650066
	-0.02	1.749887445	1.755712478	0.005825033
	0	0	0	0
	0.02	-1.749887445	-1.755712478	0.005825033
	0.04	-3.499774890	-3.511424956	0.011650066
$t = 0.06$	-0.04	4.099780218	4.169817134	0.070036916
	-0.02	2.049890109	2.084908567	0.035018458
	0	0	0	0
	0.02	-2.049890109	-2.084908567	0.035018458
	0.04	-4.099780218	-4.169817134	0.070036916
$t = 0.08$	-0.04	4.859650332	5.132082627	0.272432295
	-0.02	2.429825166	2.566041313	0.136216147
	0	0	0	0
	0.02	-2.429825166	-2.566041313	0.136216147
	0.04	-4.859650332	-5.132082627	0.272432295
$t = 0.10$	-0.04	5.807054134	6.671707415	0.864653281
	-0.02	2.903527067	3.335853708	0.432326641
	0	0	0	0
	0.02	-2.903527067	-3.335853708	0.432326641
	0.04	-5.807054134	-6.671707415	0.864653281

As occurred in the first two problems, the data in Table 3 indicate that the absolute error progressively becomes worse as the value of t increases. It was discovered that the error initially increases from 0 to an order that significantly increases from $\times 10^{-2}$ to $\times 10^{-1}$.

$$\mu(x, t) = \lim_{n \rightarrow \infty} \mu_n(x, t);$$

$$\frac{h^2}{6} \partial R_\theta^3 + \frac{3}{2\sqrt{gh}} R \partial R_\theta + \partial R_\varphi = 0. \tag{82}$$

therefore, the closed form of Eq. (64) is obtained as:

$$\mu(x, t) = \frac{x}{1 + \xi t}, \tag{81}$$

which is the exact solution.

They applied the transformation $R(\theta, \varphi) = -\frac{\sqrt{16gh^7}}{\sqrt[3]{6}} \mu(x, t)$ to reduce Eq. (82) to canonical KDV equation presented as:

$$\frac{\partial^\alpha \mu(x, t)}{\partial t^\alpha} - 6\mu(x, t) \frac{\partial \mu(x, t)}{\partial x} + \frac{\partial^3 \mu(x, t)}{\partial x^3} = 0. \tag{83}$$

3.5 Application to oceanography

The mathematical model of shallow water waves in dimensional form described in [24] to clarify the disturbance caused by waves in the ocean bottom is:

Let the initial condition be:

$$\mu(x, 0) = x. \tag{84}$$

Then, Eq. (83) becomes a particular case of Eq. (65) when $\xi = -6$, such that

$$\mu_n(x, t) = x + 6tx + 36t^2x + 216t^3x + \dots, \tag{85}$$

and

$$\mu(x, t) = \frac{x}{1 - 6t}. \tag{86}$$

3.6 Numerical simulation

Here, we conduct a numerical simulation of the disturbance caused by water waves in the domain of shallow water described by $R(x, t) = \{(x, t) | -0.05 \leq x \leq 0.05, 0 < t < 0.42\}$. Equation (86) is substituted into the transformation $R(\theta, \varphi) = -\frac{\sqrt{16gh^{\frac{7}{6}}}}{\sqrt[3]{6}}\mu(x, t)$ to obtain the theoretical solution of Eq. (82).

$$R(\theta, \varphi) = -\frac{\sqrt{16gh^{\frac{7}{6}}}}{\sqrt[3]{6}}\left(\frac{x}{1 - 6t}\right) \tag{87}$$

Also, Eq. (85) is substituted into $R(\theta, \varphi)$ such that the following numerical solution is obtained (Fig. 3, Table 3)

$$-\frac{\sqrt{16gh^{\frac{7}{6}}}}{\sqrt[3]{6}}(x + 6tx + 36t^2x + 216t^3x + \dots) \tag{88}$$

3.7 Theoretical perspective

Physical problems are well modeled with the aid of the Caputo derivative concept. This study reveals that its differentials are powerful tools for modeling linear and nonlinear systems where the order affects the output of functional parameters they contain. The impact of wave interference on nature is determined by the amount of wave crest that forms, which is referred to as “Frequency.” The analysis conducted with the aid of the Caputo derivative employed in this research reveals that the crests formed by water waves are always maximum at an integer-order derivative. This integer order represents a situation in which a water wave is directly propagating in a region with no feasible obstructions. This direct propagation can result in ocean floor landslides and the redistribution of sand and sediment in coastal areas. This can potentially lead to environmental hazards such as flooding and erosion, and the end results are often the loss of life and damage to the properties of people living in coastal regions. To avoid wind-generated waves, direct propagation of winds into the water should be kept to a minimum, which can

be accomplished by embracing environmental aiding techniques such as tree planting (which acts as a wind-breaker). Other options for controlling water waves include the construction of groins along the shoreline, jetties along coastal lines, and breakwater barriers along the shoreline.

4 Discussion

Unlike previous numerical methods, which required several iterations and tedious computational work to achieve convergence, the proposed method is effective and faster and requires less computation time to obtain the approximate solitons of the fractional-order KDV equation. In a similar but different study presented in [14], the effectiveness of Caputo differentials was seen. It was applied as one of their operators to provide a computational approach for solving shallow water KDV equations. They achieved this by blending the Caputo derivative with a numerical technique that combines the q-homotopy analysis transform technique and the Laplace transform method, although the objectives of their research extend to hiring two other fractional derivatives named “Caputo–Fabrizio” and “Atangana–Baleanu” to show their impact in generalizing mathematical models associated with power law, non-locality, singularity, and non-singularity kernels. In this study, this same Caputo operator proved that it cannot be overridden when it comes to modeling non-localized phenomena. It shares an accurate insight into wave properties and behavior through numerical simulation. A major limitation of computing fractional-order derivatives is its restriction to a few symbolic software packages such as the Mathematica software package; hence, it is recommended that laptops with the minimum specifications: Disk Space: 19 GB; System Memory (RAM): 4 GB+, are applied to ensure high computation speed [10].

5 Conclusion

In this research, we proposed an analytical way of solving the fractional-order Korteweg–de Vries equation. The method was derived by coupling an initial guess technique with He’s homotopy perturbation method. The new method was applied to different KDV equations with Caputo fractional derivatives. The approximate solution obtained gives a series solution in fractional order, which accelerates rapidly to the exact solution at an integer order. A conceptual study of the fractional-order derivative in wave dispersion was carried out by simulating the approximate traveling wave solution and investigating the disturbance caused by waves in the shallow water domain using the MAPLE 18 software. The outcome, which was extensively discussed, reveals the significant impact of

Caputo's fractional-order derivative in wave dispersion and propagation, and it also gives insight on ways of controlling wave-associated hazards.

Abbreviations

KDV: Korteweg–de Vries; MIGHPM: Modified initial guess homotopy perturbation method; LADM: Laplace–Adomian decomposition; HPM: Homotopy perturbation method; DTM: Differential transform method; FDTM: Fractional differential transform method; MDTM: Modified differential transform method.

Acknowledgements

The efforts of all academic colleagues in the department of Mathematical sciences of Osun State university, Osogbo, are acknowledged.

Author contributions

All contributed to method development; MOO was involved in problems formulation; KAA contributed to computation; JAA was involved in results simulation; and AOO contributed to typesetting and proof reading. All authors read have read and approved the manuscript.

Funding

No funding has been received.

Availability of data and materials

Not applicable.

Declarations

Ethics approval and consent to participate

Not applicable.

Consent for publication

Not applicable.

Competing interests

The authors declare that there are no competing interests.

Received: 15 July 2022 Accepted: 27 October 2022

Published online: 02 December 2022

References

- Aghili A (2017) Non-homogeneous KdV and coupled sub-ballistic fractional PDEs. *New Trends Math Sci* 5(3):107–117. <https://doi.org/10.20852/ntmsci.2017.189>
- Appadu AR, Kelil AS (2020) On semi-analytical solutions for linearized dispersive KdV equations. *Mathematics* 8:1769. <https://doi.org/10.3390/math8101769>
- Atangana A, Baleanu D (2016) New fractional derivatives with non-local and nonsingular kernel theory and application to heat transfer model. *Therm Sci* 20:763–769
- Baleanu D, Etemad S, Rezapour S (2020) A hybrid Caputo fractional modeling for thermostat with hybrid boundary value conditions. *Bound Value Probl*. <https://doi.org/10.1186/s13661-020-01361-0>
- Baleanu D, Mohammadi H, Rezapour S (2020) Analysis of the model of HIV-1 infection of CD4+ T-cell with a new approach of fractional derivative. *Adv Differ Equ*. <https://doi.org/10.1186/s13662-020-02544-w>
- Baleanu D, Mohammadi H, Rezapour S (2020) A mathematical theoretical study of a particular system of Caputo-Fabrizio fractional differential equations for the Rubella disease model. *Adv Differ Equ*. <https://doi.org/10.1186/s13662-020-02614-z>
- Biazar J, Ghazvini H (2009) Convergence of the homotopy perturbation method for partial differential equations. *Nonlinear Anal Real World Appl* 10:2633–2640
- Bird EC (1996) *Coastal erosion and rising sea-level*. Springer, Dordrecht, pp 87–103
- Biswas A, Konar S, Zerrad E (2007). Soliton perturbation theory for the splitted regularized long wave equation. *Adv Stud Theor Phys* 1
- Bonyah E, Yavuz M, Baleanu D, Kumar S (2022) A robust study on the lysteriosis disease by adopting fractal-fractional operators. *Alex Eng J* 61(3):2016–2028. <https://doi.org/10.1016/j.aej.2021.07.010>
- Boussinesq J (1872) Théorie des ondes et des remous qui se propagent le long d'un canal rectangulaire horizontal en communiquant au liquide contenu dans ce canal des vitesses sensiblement pareilles de la surface au fond. *J Math Pures Appl* 55–108. <http://eudml.org/doc/234248>
- Brent JL, Onder EN, Prudil AA (2022) Chapter 12: Nonlinear differential equations. In: *Advanced mathematics for engineering students*. Butterworth-Heinemann, Oxford, pp 329–347. <https://doi.org/10.1016/B978-0-12-823681-9.00020-4>
- Caputo M (1969) *Elasticita e Dissipazione*. Zanichelli, Bologna
- Caputo M, Fabrizio M (2016) A new definition of fractional derivative without singular kernel. *Prog Fract Differ Appl* 1(2):73–85
- Craik ADD (2004) The origin of water waves theory. *Ann Rev Fluid Mech* 36:1–28
- Debnath L (1997) *Nonlinear partial differential equations for scientists and engineers*. Birkhäuser, Boston. <https://doi.org/10.1007/978-1-4899-2846-7>
- Drazin PG, Johnson RS (1989) *Solitons: an introduction*. Cambridge University Press, Cambridge. <https://doi.org/10.1017/CBO9781139172059>
- Emile F, Goufo D (2021) On the fractal dynamics for higher order traveling waves. *Chaos Solitons Fractals*. <https://doi.org/10.1016/j.chaos.2021.111059>
- Hammouch Z, Yavuz M, Özdemir N (2021) Numerical solutions and synchronization of a variable-order fractional chaotic system. *Math Model Numer Simul Appl* 1:11–23. <https://doi.org/10.53391/mmnsa.2021.01.002>
- Haq F, Shah K, Rahman G, Shahzad M (2017) Numerical solution of fractional order smoking model via Laplace adomian decomposition method. *Alex Eng J*. <https://doi.org/10.1016/j.aej.2017.02.015>
- He JH (1999) Variational iteration method—a kind of non-linear analytical technique: some examples. *Int J Non-Linear Mech* 34(4):699–708. [https://doi.org/10.1016/S0020-7462\(98\)00048-1](https://doi.org/10.1016/S0020-7462(98)00048-1)
- He JH (1999) Homotopy perturbation technique. *Comput Methods Appl Mech Eng* 178:257–262
- He JH (2005) Homotopy perturbation method for bifurcation of nonlinear problems. *Int J Nonlinear Sci Numer Simul* 6(2):207–208. <https://doi.org/10.1515/IJNSNS.2005.6.2.207>
- He JH (2006) Some asymptotic methods for strongly nonlinear equations. *Int J Mod Phys B* 20:1141–1199
- He JH, El-dib Y, Mady AA (2021) Homotopy perturbation method for the fractal toda oscillator. *Fractal Fract* 5:93. <https://doi.org/10.3390/fractalfract5030093>
- Helal MA, El-Eissa HN (1996) Shallow water waves and Korteweg de Vries equation (oceanographical application). *Pure Math Appl* 7(3):263–282
- Jhangeer A, Faridi WA, Asjad MI, Inc M (2022) A comparative study about the propagation of water waves with fractional operators. *J Ocean Eng Sci*. <https://doi.org/10.1016/j.joes.2022.02.010>
- Konno K, Ichikawa HY (1974) A modified Korteweg de Vries equation for ion acoustic waves. *J Phys Soc Jpn* 37(6):1631–1636
- Korteweg DJ, de Vries G (1895) On the change of form of long waves advancing in a rectangular canal, and on a new type of long stationary waves. *Philos Mag* 5(39):422–443
- Miles J (1981) The Korteweg-de Vries equation: a historical essay. *J Fluid Mech* 106:131–147. <https://doi.org/10.1017/S0022112081001559>
- Muhammad F, Saleem MU, Ahmad A, Ahmad MO (2018) Analysis and numerical solution of SEIR epidemic model of measles with non-integer time fractional derivatives by using Laplace adomian decomposition method. *Ain Shams Eng J*. <https://doi.org/10.1016/j.aej.2017.11.010>
- Olayiwola MO (2013) On a modified variational iteration method for the analytical solution of Korteweg-de-Vries equation 25:467–470
- Olayiwola MO, Gbolagade AW, Adesanya AO (2010) Solving variable coefficient fourth-order parabolic equation by modified initial guess variational iteration method. *J Niger Assoc Math Phys* 16:205–210
- Olayiwola MO, Gbolagade AW, Adesanya AO (2010) An efficient algorithm for solving the telegraph equation. *J Niger Assoc Math Phys* 16:199–204
- Olayiwola MO, Gbolagade AW, Akinpelu FO (2011) An efficient algorithm for solving the nonlinear PDE. *Int J Sci Eng Res* 2:1–10

36. Ravi Kant ASV, Aruna K (2015) Solution of fractional third-order dispersive partial differential equations. *Egypt J Basic Appl Sci* 2(3):190–199. <https://doi.org/10.1016/j.ejbas.2015.02.002>
37. Seadawy AR (2011) New exact solutions for the KdV equation with higher order nonlinearity by using the variational method. *Comput Math Appl* 62(10):3741–3755. <https://doi.org/10.1016/j.camwa.2011.09.023>
38. Shah R, Khan H, Arif M, Kumam P (2019) Application of Laplace-Adomian decomposition method for the analytical solution of third-order dispersive fractional partial differential equations. *Entropy* 21(4):335. <https://doi.org/10.3390/e21040335>
39. Shanmugam G (2006) The Tsunami problem. *J Sediment Res* 76:718–730. <https://doi.org/10.2110/jsr.2006.073>
40. System requirement for mathematical software (2022). <https://www.wolfram.com/mathematica/system-requirements.html>
41. Veerasha P, Yavuz M, Baishya C (2021) A computational approach for shallow water forced Korteweg–De Vries equation on critical flow over a hole with three fractional operators. *Int J Optim Control Theor Appl (IJOCTA)* 11:52–67
42. Vreugdenhil CB (1994) Three-dimensional shallow-water flow. In: Numerical methods for shallow-water flow. Water Science and Technology Library. Springer, Dordrecht, p 13. https://doi.org/10.1007/978-94-015-8354-1_11
43. Wazwaz AM (2003) An analytic study on the third-order dispersive partial differential equations. *Appl Math Comput* 142:511–520. [https://doi.org/10.1016/S0096-3003\(02\)00336-3](https://doi.org/10.1016/S0096-3003(02)00336-3)
44. Yokuş A (2021) Construction of different types of traveling wave solutions of the relativistic wave equation associated with the Schrödinger equation. *Math Model Numer Simul Appl* 1(1):24–31. <https://doi.org/10.53391/mmnsa.2021.01.003>
45. Yong Y, Li Y, Jin Y, Shen H (2015) Simulation of shallow-water waves in coastal region for marine simulator

Publisher's Note

Springer Nature remains neutral with regard to jurisdictional claims in published maps and institutional affiliations.

Submit your manuscript to a SpringerOpen[®] journal and benefit from:

- ▶ Convenient online submission
- ▶ Rigorous peer review
- ▶ Open access: articles freely available online
- ▶ High visibility within the field
- ▶ Retaining the copyright to your article

Submit your next manuscript at ▶ [springeropen.com](https://www.springeropen.com)
